Journal of Al-Nahrain University Vol.13 (2), June, 2010, pp.105-113 Science

NUCLEON MOMENTUM DISTRIBUTIONS AND ELASTIC ELECTRON SCATTERING DIFFERENTIAL CROSS SECTIONS FOR SOME *2s-1d* SHELL NUCLEI

A.K. Hamoudi
Department of Physics, College of Science, University of Baghdad, Baghdad-Iraq.

Abstract

The nucleon momentum distributions for the ground state and elastic electron scattering differential cross sections have been calculated in the framework of the coherent fluctuation model and expressed in terms of the weight function (fluctuation function). The weight function has been related to the nucleon density distributions of nuclei and determined from theory and experiment. The feature of long-tail behavior at high momentum region of the nucleon momentum distributions has been obtained using both theoretical and experimental weight functions. An A-dependence of the nucleon momentum distributions has been clearly found in the region of high momentum component $k \geq 3\, fm^{-1}$. The observed differential cross sections for electron scattering from ^{20}Ne, ^{24}Mg, ^{28}Si and ^{32}S nuclei are very well reproduced by the present calculations throughout all values of scattering angle θ.

Keywords: Nucleon density distributions, Nucleon momentum distributions, Elastic electron scattering differential cross sections and *2s-1d* shell nuclei.

Introduction

There is no method for directly measuring the nucleon momentum distribution (*NMD*) in nuclei. The quantities that are measured by particle-nucleus and nucleus-nucleus collisions are the cross sections of different reactions, and these contain information on the *NMD* of target nucleons. The experimental evidence obtained from inclusive and exclusive electron scattering on nuclei established the existence of long-tail behavior of the *NMD* at high momentum region ($k \geq 2\, fm^{-1}$) [1-6]. In principle, the mean field theories cannot describe correctly the form factors $F(q)$ and the *NMD* simultaneously [7] and they exhibit a steep-slope behavior of the *NMD* at high momentum region. In fact, the *NMD* depends a little on the effective mean field considered due to its sensitivity to the short-range and tensor nucleon-nucleon correlations [7, 8] which are not included in the mean field theories.

There are several theoretical methods used to study elastic electron-nucleus scattering, such as the plan-wave Born approximation (PWBA), the eikonal approximation and the phase-shift analysis method [9-15]. The PWBA method can give qualitative results and has been used widely for its simplicity. To include the Coulomb distortion effect, which is neglected in PWBA, the other two methods may be used. In the past few years, some theoretical studies of elastic electron scattering off exotic nuclei have been performed. Wang et al. [11, 12] studied such scattering along some isotopic and isotonic chains by combining the eikonal approximation with the relativistic mean field theory. And, very recently, Roca-Maza et al. [13] systematically investigated elastic electron scattering off both stable and exotic nuclei with the phase-shift analysis method. Karataglidis and Amos [14] have studied the elastic electron scattering form factors, longitudinal and transverse, from exotic (*He* and *Li*) isotopes and from ^{8}B nucleus using large space shell model functions. Very recently, Chu et al. [15] have studied the elastic electron scattering along O and S isotopic chains and shown that the phase-shift analysis method can reproduce the experimental data very well for both light and heavy nuclei.

In the coherent fluctuation model (*CFM*), which is exemplified by the work of Antonov et. al. [4, 16], the local nucleon density distribution (*NDD*) and the *NMD* are simply related and expressed in terms of an

experimentally obtainable fluctuation function (weight function) $|f(x)|^2$. They [4, 16] investigated the *NMD* of (^4He and ^{16}O), ^{12}C and (^{39}K, ^{40}Ca and ^{48}Ca) nuclei using weight functions $|f(x)|^2$ expressed in terms of, respectively, the experimental two parameter Fermi ($2PF$) *NDD* [17], the experimental data of Ref. [18] and the experimental model-independent *NDD* [17]. It is important to point out that all above calculations obtained in the framework of the *CFM* proved a high momentum tail in the *NMD*. Elastic electron scattering from ^{40}Ca nucleus was also investigated in Ref. [16], where the calculated elastic differential cross sections ($d\sigma/d\Omega$) were found to be in good agreement with those of experimental data.

The aim of the present work is to derive an analytical form for the *NDD* applicable throughout all $2s-1d$ shell nuclei based on the use of the single particle harmonic oscillator wave functions and the occupation numbers of the states. The derived *NDD* is employed in determining the theoretical weight function $|f(x)|^2$ which is used in the *CFM* to study the *NMD* and elastic differential cross sections $d\sigma/d\Omega$ for some $2s-1d$ shell nuclei, such as ^{20}Ne, ^{24}Mg, ^{28}Si and ^{32}S nuclei. We shall see later that the theoretical $|f(x)|^2$, based on the derived *NDD*, is capable to give information about the *NMD* and $d\sigma/d\Omega$ as the experimental $|f(x)|^2$, based on the three parameter Fermi (*3PF*) *NDD* [17, 19], does.

Theory

In the *CFM* [4, 16], the mixed density is given by

$$\rho(r,r') = \int_0^\infty |f(x)|^2 \rho_x(r,r')dx \quad \text{.....(1)}$$

where [4, 16]

$$\rho_x(r,r') = 3\rho_0(x)\frac{j_1(k_F(x)|\vec{r}-\vec{r}'|)}{k_F(x)|\vec{r}-\vec{r}'|} \times \theta\left(x-\frac{|\vec{r}+\vec{r}'|}{2}\right) \quad \text{.....(2)}$$

is the density matrix for A nucleons uniformly distributed in the sphere with radius x and density $\rho_0(x) = 3A/4\pi x^3$. The Fermi momentum is defined as [4, 16].

$$k_F(x) = \left(\frac{3\pi^2}{2}\rho_0(x)\right)^{1/3} = \left(\frac{9\pi A}{8}\right)^{1/3}\frac{1}{x} = \frac{\alpha}{x}; \qquad \alpha = \left(\frac{9\pi A}{8}\right)^{1/3} \quad \text{.....(3)}$$

and the step function θ is defined by

$$\theta(y) = \begin{cases} 1, & y \geq 0 \\ 0, & y < 0 \end{cases} \quad \text{.....(4)}$$

Equation (1) corresponds to the general statement of the *CFM* in which the nuclear matter *NDD* fluctuates around the average distribution, keeping spherical symmetry and uniformity. The diagonal element of (1) gives the one-particle density as

$$\rho(r) = \rho(r,r'=r) = \int_0^\infty |f(x)|^2 \rho_x(r)dx \quad \text{.....(5)}$$

In (5), $\rho_x(r)$ and $|f(x)|^2$ have the following forms [16]

$$\rho_x(r) = \rho_0(x)\theta\left(x-|\vec{r}|\right) \quad \text{.....(6)}$$

$$|f(x)|^2 = -\frac{1}{\rho_0(x)}\frac{d\rho(r)}{dr}\Big|_{r=x} \quad \text{.....(7)}$$

The weight function $|f(x)|^2$ of (7), determined in terms of the *NDD* $\rho(r)$, satisfies the normalization condition

$$\int_0^\infty |f(x)|^2 dx = 1 \quad \text{.....(8)}$$

and holds only for monotonically decreasing *NDD*, i.e. $\frac{d\rho(r)}{dr} < 0$.

On the basis of (5), the *NMD*, $n(k)$, is expressed as [16]

$$n(k) = \int_0^\infty |f(x)|^2 n_x(k)dx \quad \text{.....(9)}$$

where

$$n_x(k) = \frac{4}{3}\pi x^3\theta\left(k_F(x)-|\vec{k}|\right) \quad \text{.....(10)}$$

is the Fermi-momentum distribution of the system with density $\rho_0(x)$. By means of (7), (9) and (10), an explicit form for $n(k)$ is expressed in terms of $\rho(r)$ as

$$n(k)=\left(\frac{4\pi}{3}\right)^2\frac{4}{A}\times\left[6\int_0^{\alpha/k}\rho(x)x^5dx-\left(\frac{\alpha}{k}\right)^6\rho\left(\frac{\alpha}{k}\right)\right] \quad \ldots\ldots(11)$$

with normalization condition

$$\int n(k)\frac{d^3k}{(2\pi)^3}=A$$

The NMD of $2s-1d$ shell nuclei is also determined by the shell model using the single particle harmonic oscillator wave function in momentum representation and is given by [6]

$$n(k)=\frac{4b^3}{\pi^{3/2}}\exp(-\frac{b^2}{k^2})\times\left[1+2(bk)^2+\frac{(A-16)}{15}(bk)^4\right] \quad \ldots\ldots(12)$$

where b is the harmonic oscillator size parameter.

The form factor $F(q)$ of the nucleus is also expressed in the CFM and is given by [16]

$$F(q)=\frac{1}{A}\int|f(x)|^2\,F(x,q)dx \quad \ldots\ldots(13)$$

where $F(x,q)$ is the form factor of uniform charge density distribution given by

$$F(x,q)=\frac{3A}{(qx)^2}\left[\frac{\sin(qx)}{qx}-\cos(qx)\right] \quad \ldots(14)$$

Equation (14) reflects the physical scattering picture, inherent by the CFM, in which the scattering amplitude is a superposition of different uniform charge distributions. The nucleon finite size (fs) form factor is defined by $F_{fs}(q)=Exp(-0.43q^2/A)$ [10] and $F_{cm}(q)=Exp(q^2b^2/4A)$ is the correction for the lack of translational invariance in the shell model (center of mass correction) [10]. Inclusion of $F_{fs}(q)$ and $F_{cm}(q)$ in the calculations requires multiplying the form factor of (13) by these corrections.

It is important to point out that all physical quantities studied above in the framework of the CFM such as $n(k)$ and $F(q)$ are expressed in terms of the weight function $|f(x)|^2$. Therefore, it is worthwhile trying to obtain the weight function firstly from the NDD of the $3PF$ model extracted from the analysis of elastic electron-nuclei scattering experiments and secondly from theoretical considerations. The NDD of the $3PF$ model is given by [17]

$$\rho_{3PF}(r)=\rho_0\left(1+\frac{wr^2}{c^2}\right)\Big/\left(1+e^{\frac{r-c}{z}}\right);\qquad \rho_0=\frac{A}{4\pi}\frac{1}{\int_0^\infty\left(1+\frac{wr^2}{c^2}\right)\left(1+e^{\frac{r-c}{z}}\right)^{-1}r^2dr} \quad \ldots\ldots(15)$$

The weight function $|f(x)|^2_{3PF}$ is obtained by introducing (15) into (7) as

$$|f(x)|^2_{3PF}=\frac{4\pi x^3}{3A}\frac{1}{e^{\frac{x-c}{z}}}\times\left\{\frac{1}{z}\rho_{3PF}(x)e^{\frac{x-c}{z}}-\frac{2}{c^2}\rho_0 wx\right\} \quad \ldots\ldots(16)$$

Theoretically, the NDD of one body operator can be written as [20]

$$\rho(r)=\frac{1}{4\pi}\sum_{nl}\zeta_{nl}4(2l+1)\phi^*_{nl}(r)\phi_{nl}(r) \quad \ldots\ldots(17)$$

Here ζ_{nl} is the nucleon occupation probability of the state nl ($\zeta_{nl}=0$ or 1 for closed shell nuclei and $0<\zeta_{nl}<1$ for open shell nuclei) and $\phi_{nl}(r)$ is the radial part of the single particle harmonic oscillator wave function.

To derive an explicit form for the NDD of $2s-1d$ shell nuclei, we follow the method of [9] and assume that there is a core of filled $1s$ and $1p$ shells and the nucleon numbers in $2s$ and $1d$ shells are equal to, respectively, $4-\delta$

and $A-20+\delta$, and not to 4 and $A-20$ as in the simple shell model. Using this assumption with the help of (17), an analytical form for $\rho(r)$ is obtained as

$$\rho(r)=\frac{e^{-r^2/b^2}}{\pi^{3/2}b^3}\left\{10-\frac{3\delta}{2}+\frac{2\delta r^2}{b^2}+\left(\frac{4A}{15}-\frac{8}{3}-\frac{2\delta}{5}\right)\frac{r^4}{b^4}\right\} \quad \ldots.(18)$$

Here, the parameter δ characterizes the deviation of the nucleon occupation numbers from the prediction of the simple shell model ($\delta=0$). The central NDD, $\rho(0)$, is obtained from (18) as

$$\rho(0)=\frac{1}{\pi^{3/2}b^3}\left\{10-\frac{3\delta}{2}\right\} \quad \ldots\ldots\ldots\ldots(19)$$

Therefore, δ can be obtained from (19) as

$$\delta=\frac{2}{3}\left\{10-\pi^{3/2}b^3\rho(0)\right\} \quad \ldots\ldots\ldots\ldots(20)$$

Using (18) in (7), an analytical expression for theoretical weight function $|f(x)|^2$ is obtained as

$$|f(x)|^2=\frac{8\pi}{3Ab^2}x^4\rho(x)-\frac{32}{3A\pi^{1/2}b^5}x^4\times e^{-x^2/b^2}\left\{\delta+\left(\frac{4Z}{15}-\frac{4}{3}-\frac{2\delta}{5}\right)\frac{x^2}{b^2}\right\} \quad \ldots\ldots\ldots\ldots(21)$$

Results and Discussion

The nucleon momentum distributions $n(k)$ and elastic differential cross section $d\sigma/d\Omega$ for $2s-1d$ shell nuclei are studied by means of the CFM. The distribution $n(k)$ of (9) is calculated in terms of the weight function obtained firstly from the fit to the electron-nuclei scattering experiments, as in (16), and secondly from theory, as in (21). The harmonic oscillator size parameters b are chosen in such a way as to reproduce the measured root mean square radii (rms) of nuclei. The parameters δ are determined by introducing the chosen values of b and the experimental densities $\rho_{exp}(0)$ into (20). The values of b and δ together with the other parameters employed in the present calculations for ^{20}Ne, ^{24}Mg, ^{28}Si and ^{32}S nuclei are listed in Table 1. The calculated rms $\langle r^2\rangle_{cal}^{1/2}$ and those of experimental data $\langle r^2\rangle_{exp}^{1/2}$ [17, 19] are displayed in this table as well for comparison. The comparison shows a remarkable agreement between $\langle r^2\rangle_{cal}^{1/2}$ and $\langle r^2\rangle_{exp}^{1/2}$ for all considered nuclei. The dependence of the $n(k)$ (in fm^3) on k (in fm^{-1}) for ^{20}Ne, ^{24}Mg, ^{28}Si and ^{32}S nuclei is shown in Fig.(1). The dash-dotted distributions are the NMD's of (12) obtained by the shell model calculation using the single particle harmonic oscillator wave functions in the momentum representation. The dotted and solid distributions are the NMD's obtained by the CFM and expressed in terms of the experimental and theoretical weight functions (16) and (21), respectively. It is clear that the behavior of the dash-dotted distributions reproduced by the shell model calculations is in contrast with those of the dotted and solid distributions reproduced by the CFM. The important feature of the dash-dotted distributions is the steep slope behavior when k increases. This behavior is in disagreement with other studies [4, 5, 7, 8] and it is attributed to the fact that the ground state shell model wave functions given in terms of a Slater determinant does not take into account the important effects of the short range dynamical correlation functions. Hence, the short-range repulsive features of the nucleon-nucleon forces are responsible for the high momentum behavior of the NMD [5, 7]. It is seen that the dotted and solid distributions deviate slightly from each other around the region of momentum $k\geq 3\,fm^{-1}$. It is also noted that the general structure of the dotted and solid distributions at the region of high momentum components is almost the same for ^{20}Ne, ^{24}Mg, ^{28}Si and ^{32}S nuclei, where these distributions have the feature of long-tail behavior at momentum region $k\geq 2\,fm^{-1}$. In fact, the feature of long-tail behavior obtained by the CFM, which is in agreement with other studies [4, 5, 7, 8], is related to the existence of high densities $\rho_x(r)$ in the decomposition (5), though their weight functions $|f(x)|^2$ are small. The mass

dependence of the *NMD*, calculated by means of the *CFM* using the theoretical weight function (21), is studied and analyzed in Fig.(2). The solid, dotted, dash-dotted and dashed distributions are the *NMD*'s for ^{20}Ne, ^{24}Mg, ^{28}Si and ^{32}S nuclei, respectively. It is obvious that there is an A-dependence in $n(k)$, which is in agreement with the study of Ref. [5], especially at the region of high momentum component $k \geq 3\ fm^{-1}$ while at the region of small values of k this dependence is quite small as shown in Fig.(2). Elastic differential cross sections, defined by $d\sigma/d\Omega = (d\sigma/d\Omega)_{Mott} \times |F(q)|^2$ [10], are also studied by means of the *CFM*. Here, $(d\sigma/d\Omega)_{Mott}$ is the Mott cross section for relativistic electron scattering from a point charge and $F(q)$ is the form factor given by (13). The present results for elastic differential cross sections $d\sigma/d\Omega$ are plotted versus the scattering angle θ for ^{20}Ne, ^{24}Mg, ^{28}Si and ^{32}S nuclei as shown in Fig.3. The solid and dotted curves are the calculated results obtained, respectively, without and with including the corrections of $F_{fs}(q)$ and $F_{cm}(q)$. In ^{20}Ne nucleus, the symbols of solid circles, solid squares, solid triangles and bolded pluses are the experimental data of elastic differential cross sections $d\sigma/d\Omega$ [21] for energies $39.94 MeV$, $65.93 MeV$, $114.93 MeV$ and $119.93 MeV$, respectively. It is clear that the experimental data [21] are extremely well reproduced by both calculations of the solid and dotted curves throughout all values of θ. The effect of including $F_{fs}(q)$ and $F_{cm}(q)$ corrections in the calculations of the ^{20}Ne nucleus is insignificant because it leads to slight reduction in the calculated cross sections throughout all values of θ as seen by the dotted curves. In ^{24}Mg, ^{28}Si and ^{32}S nuclei, the symbols of opened circles and opened triangles are the experimental data of elastic differential cross sections $d\sigma/d\Omega$ [19] for energies $250 MeV$ and $500 MeV$, respectively. The general structure for both behavior and magnitude of the calculated cross sections represented by the solid and dotted curves are in very good agreement with those of experimental data. All the first diffraction minima in the energy region $250 MeV$ and all first and second diffraction minima in the energy region $500 MeV$ are reproduced in the correct places. The inclusion of the nucleon finite size and center of mass corrections in the calculations of these nuclei reduces the magnitudes of the calculated $d\sigma/d\Omega$ clearly around the region of $\theta \geq 60$ as seen by the dotted curves. It is obvious that the solid curves in ^{24}Mg, ^{28}Si and ^{32}S nuclei describe the experimental data for elastic differential cross sections $d\sigma/d\Omega$ [19] better than the dotted curves throughout all values of θ.

Summary and Conclusions

The *NMD* and elastic differential cross sections calculated in the framework of the *CFM* were expressed by means of the weight function $|f(x)|^2$. The weight function, which is connected with the local density $\rho(r)$, was determined from experiment, as in (16), and from theory, as in (21). The feature of the long-tail behavior of the *NMD*, which is in accordance with the other studies [4, 5, 7, 8], is obtained by both theoretical and experimental weight functions and is related to the existence of high densities $\rho_x(r)$ in the decomposition (5), though their weight functions are small. An A-dependence of the *NMD* is clearly found at the region of high momentum component $k \geq 3\ fm^{-1}$ and is slightly seen at the region of small values of k. The mass dependence of the *NMD*, which is found in the present study, agrees with that found in the study of Ref. [5]. The observed differential cross sections for elastic electron scattering from ^{20}Ne, ^{24}Mg, ^{28}Si and ^{32}S nuclei are very well reproduced by the present calculations of the *CFM* throughout all values of scattering angle θ. It is noted that the theoretical *NDD* (18) employed in the determination of the theoretical weight function (21) is capable of reproducing the information about the *NMD* and elastic differential cross sections as does the *3PF* model.

Table (1)
The values of various parameters employed in the present calculations together with $\langle r^2 \rangle_{cal}^{1/2}$ *and* $\langle r^2 \rangle_{exp}^{1/2}$.

Nuclei	3PF [17, 19]			Experimental central NDD [17, 19]	Calculated parameters and rms of the present work			Experimental rms [17, 19]
	w	c (fm)	z (fm)	$\rho_{exp}(0)$ (fm^{-3})	b (fm)	δ	$\langle r^2 \rangle_{cal}^{1/2}$ (fm)	$\langle r^2 \rangle_{exp}^{1/2}$ (fm)
^{20}Ne	-.168	2.791	0.698	0.1761	1.848	2.538	2.912	2.992 ± 0.03
^{24}Mg	-.249	3.192	0.604	0.1777	1.806	2.778	2.941	2.985 ± 0.03
^{28}Si	-.149	3.239	0.574	0.1768	1.870	2.373	3.105	3.106 ± 0.03
^{32}S	-.213	3.441	0.624	0.1816	1.924	1.862	3.237	3.239 ± 0.03

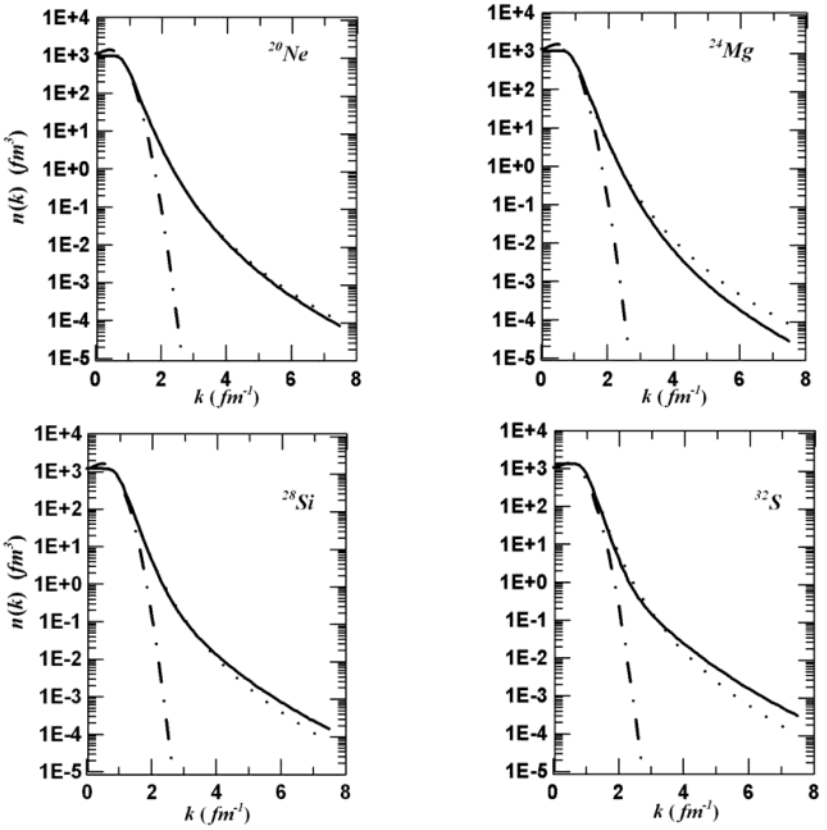

Fig.(1) : The nucleon momentum distributions (*NMD* ***'s) for*** ^{20}Ne, ^{24}Mg, ^{28}Si ***and*** ^{32}S ***nuclei. The dashed-dotted distributions are the results obtained by the shell model calculation using the single particle harmonic oscillator wave functions in the momentum representation. The dotted and solid distributions are the calculated results expressed by the*** *CFM* ***using the experimental and theoretical weight functions of (16) and (21), respectively.***

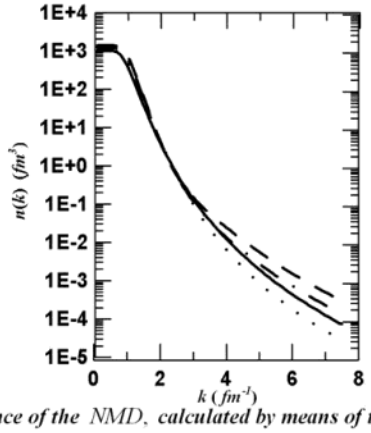

Fig.(2): The mass dependence of the NMD, calculated by means of the CFM using the theoretical weight function (21), located at the region of high momentum components $k \geq 3\ fm^{-1}$. the solid, dotted, dash-dotted and dashed curves are the calculated NMD's for ^{20}Ne, ^{24}Mg, ^{28}Si and ^{32}S nuclei, respectively.

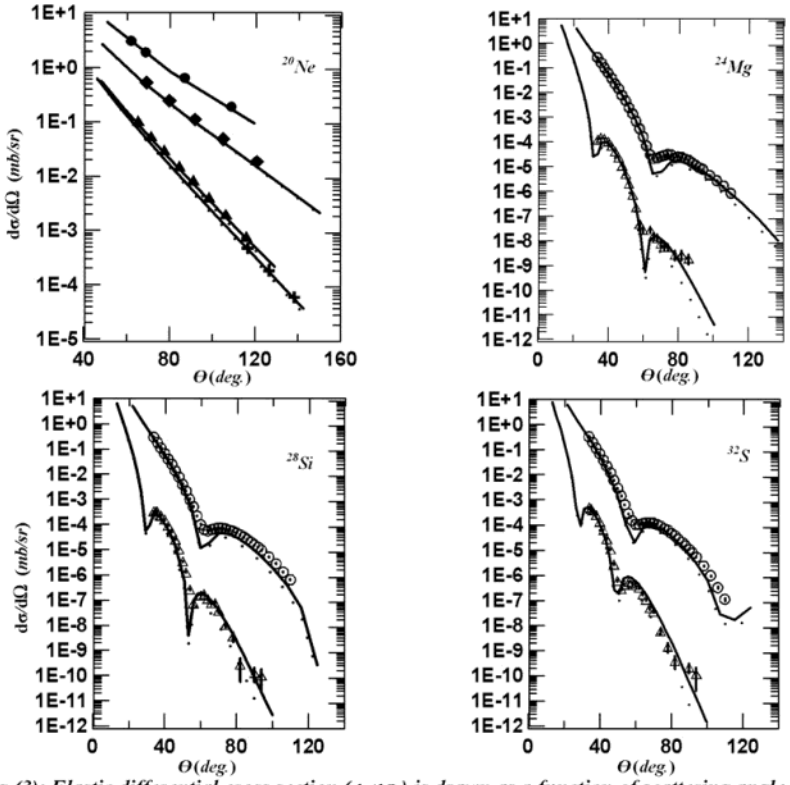

Fig.(3): Elastic differential cross section ($d\sigma/d\Omega$) is drawn as a function of scattering angle θ for ^{20}Ne, ^{24}Mg, ^{28}Si and ^{32}S nuclei. The solid and dotted curves are the calculated results without and with including the corrections (nucleon finite size and center of mass corrections), respectively. In ^{20}Ne nucleus, the symbols of solid circles, solid squares, solid triangles and bolded pluses are the experimental data, taken from Ref. [21], for energies 39.94, 65.93, 114.93 and 119.93MeV respectively. In ^{20}Ne, ^{24}Mg, ^{28}Si nuclei, the symbols of opened circles and opened triangles are the experimental data, taken from Ref. [19], for energies 250 MeV and 500MeV respectively.

References

[1] S. Frankel, W. Frati, O. Van Dyck, R. Werbeck and V. Highland, Inclusive cross sections for 180° production of high-energy protons, deuterons, and tritons in p-nucleus collisions at 600 and 800 MeV, Phys. Rev. Lett., 36, 1976, 642-651.

[2] R. D. Amado and R. M. Woloshyn, Mechanism for 180° proton production in energetic proton-nucleus collisions, Phys. Rev. Lett., 36, 1976, 1435-1443.

[3] V. I. Komarov, G. E. Kosarev, H. Muler, D. Netzband and t. Stiehler, Inclusive spectra and the angular distribution of protons emitted backwards in the interaction of 640 MeV protons with nuclei, Phys. Lett., B 69, 1977, 37-45.

[4] A., N. Antonov, P. E. Hodgson and I. Zh. Petkov, Nucleon momentum and density distribution in nuclei, Clarendon, Oxford, 1988, 1-165.

[5] Ch. C. Moustakidis and S.E. Massen, One-body density matrix and momentum distribution in s-p and s-d shell nucle, Phys. Rev., C 62, 2000, 34318_1-34318_7.

[6] A. R. Ridha, Elastic electron scattering form factors and nuclear momentum distributions in closed and open shell nuclei, M.Sc Thesis, University of Baghdad, 2006, 1-79.

[7] M. Traini and G. Orlandini, Nucleon momentum distributions in doubly closed shell nuclei, Z. Physik, A321, 1985, 479-484.

[8] M. Dal Ri, S. Stringari and O. Bohigas, Effects of short range correlations on one- and two-body properties of nuclei, Nucl. Phys., A376, 1982, 81-93.

[9] I. S. Gul'karov, M. M. Mansurov and A. A. Khomich, Charge density distribution of the 1s-1p and 1d-2s shell nuclei and filling numbers of the states, Sov. J. Nucl. Phys., 47, No. 1, 1988, 25-30.

[10] B. A. Brown, R. Radhi and B. H. Wildenthal, Electric quadrupole and hexadecupole nuclear excitations from the perspectives of electron scattering and modern shell-model theory, Phys. Rep., 101, No. 5, 1983, 313-358.

[11] Z. Wang and Z. Ren, Systematic study of charge form factors of elastic electron-nucleus scattering with relativistic eikonal approximation, Phys. Rev., C 71, 2005, 54323_1-54323_9.

[12] Z. Wang and Z. Ren and Y. Fan, Charge density distributions and charge form factors of the N=82 and N=126 isotonic nuclei, Phys. Rev., C 73, 2006, 14610_1-14610_9.

[13] X. Roca-Maza, M. Centellles, F. Salvat and X. Vinas, Theoretical study of elastic electron scattering off stable and exotic nuclei, Phys. Rev., C 78, 2008, 44332_1-44332_16.

[14] S. Karataglids and K. Amos, Electron scattering form factors from exotic nuclei, Phys. Lett., B 650, 2007, 148-151.

[15] Y. Chu, Z. Ren, T. Dong and Z.Wang, Theoretical study of nuclear charge densities with elastic electron scattering, Phys. Rev., C 79, 2009, 44313_1-44313_7.

[16] A. N. Antonov, V.A. Nikolaev, and I. Zh. Petkov, Nucleon momentum and density distributions of nuclei, Z. Physik, A297, 1980, 257-260.

[17] H. De Vries, C.W. De Jager, and C. De Vries, Atomic Data and Nuclear Data Tables, 36, 1987, 495-536.

[18] W. Reuter, G. Fricke, K. Merle, and H. Miska, Nuclear charge distribution and rms radius of ^{12}C from absolute electron scattering measurements, Phys. Rev., C 26, 1982, 806-818.

[19] G. C. Li, M.R. Yearian and I. Sick, High momentum-transfer electron scattering from ^{24}Mg, ^{27}Al, ^{28}Si and ^{32}S, Phys. Rev., C 9, No. 5, 1974, 1861-1877.

[20] S. E. Massen and Ch.C. Moustakidis, Systematic study of the effect of short range correlations on the form factors and densities of s-p and s-d shell nuclei, Phys. Rev. C 60, 1999, 24005_1-24005_13.

[21] E. A. Knight, R. P. Singhal, R. G. Arthur and M. W. S. Macauley, Elastic scattering of electrons from $^{20,\ 22}$Ne, J. Phys. G: Nucl. Phys. 7, 1981, 1115-1121.

الخلاصة

لقد تم أستخدام أنموذج التموج المتشاكه في حساب كل من توزيعات زخوم النيكليونات للحالة الأرضية والمقاطع العرضية التفاضلية للأستطارة الألكترونية المرنة وتم التعبير عنهما بدلالة دالة التموج. لقد تم التعبير عن دالة التموج بواسطة توزيعات كثافة النيكليونات وحسبت هذه الدالة من النتائج النظرية والعملية لتوزيعات كثافة النيكليونات. لقد تميزت نتائج توزيعات زخوم النيكليونات (المستندة على دالة التموج النظرية والعملية) بصفة الذيل الطويل عند منطقة الزخم العالي. أظهرت هذه الدراسة وجود اعتماد على كتلة النواة عند مركبة الزخم العالي ($k \geq 3\, fm^{-1}$) من توزيعات زخوم النيكليونات. و أظهرت ايضاً بأن نتائج المقاطع العرضية التفاضلية المرنة المحسوبة بأنموذج التموج المتشاكه تتفق تماماً مع النتائج العملية ولكل قيم زوايا الأستطارة في النوى ($^{20}Ne,\ ^{24}Mg,\ ^{28}Si,\ ^{32}S$).